Min, J. C.; Zhang, Y.; Tang, Y. C.

Article

Experimental study of wet porous sand layer air-drying characteristics

Energy Reports

Provided in Cooperation with:
Elsevier

Suggested Citation: Min, J. C.; Zhang, Y.; Tang, Y. C. (2020) : Experimental study of wet porous sand layer air-drying characteristics, Energy Reports, ISSN 2352-4847, Elsevier, Amsterdam, Vol. 6, Iss. 1, pp. 246-253,
https://doi.org/10.1016/j.egyr.2019.08.052

This Version is available at:
https://hdl.handle.net/10419/243740

Available online at www.sciencedirect.com
ScienceDirect
Energy Reports 6 (2020) 246–253
www.elsevier.com/locate/egyr

6th International Conference on Energy and Environment Research, ICEER 2019, 22-25 July, University of Aveiro, Portugal

Experimental study of wet porous sand layer air-drying characteristics

J.C. Min*, Y. Zhang, Y.C. Tang

Department of Engineering Mechanics, Tsinghua University, Beijing 100084, China

Received 4 August 2019; accepted 25 August 2019

Abstract

An experimental study has been carried out to investigate the convective air-drying characteristics of a wet sand layer. The experimental setup allows dynamic measurements of both sand layer weight and temperature, with hot air flowing towards the sand layer surface to ensure a uniform drying of it. Experiments are conducted for a 4 mm thick sand layer for three air temperatures of 45, 60 and 75 °C. The lumped parameter method is used to analyze the sand layer heat transfer. The results show that the sand layer temperature continuously increases throughout the drying process, which can be divided into three stages, i.e. the initial rapid, intermediate slow, and final rapid increase stages. There is no constant temperature stage that is often observed in water film evaporation experiment. The drying process can also be divided into three stages according to the sand layer drying rate variation, they are the increasing, constant, and decreasing rate stages, which roughly correspond to the three temperature rise stages. The lumped parameter analysis result supports that the convective heat from the hot air is used mainly for the water evaporation.

Peer-review under responsibility of the scientific committee of the 6th International Conference on Energy and Environment Research, ICEER 2019.

Keywords: Wet sand layer; Air drying; Temperature; Moisture content; Lumped parameter analysis; Biot number

1. Introduction

Porous media exist in many fields such as energy, chemical engineering, aerospace engineering, metallurgy, material engineering, and environmental science [1–3]. Convective drying of wet porous media is a complicated process that includes simultaneous heat and mass transfer and involves a variety of transport mechanisms such as conductive heat transfer, latent heat transfer accompanied by evaporation and condensation, vapor flow caused by differential pressure and diffusion, water flow induced by capillary force (e.g., [4–6]). Since a drying process is energy-intensive, study of it is of practical importance. Experimental investigations may provide a basis for better understanding the convective drying characteristics.

The objects that usually need to be dried include food, wood, and various materials and products. Hot air drying process affects not only product quality and performance but also production cost and efficiency. The energy

* Corresponding author.
E-mail address: minjc@tsinghua.edu.cn (J.C. Min).

https://doi.org/10.1016/j.egyr.2019.08.052

Peer-review under responsibility of the scientific committee of the 6th International Conference on Energy and Environment Research, ICEER 2019.

Nomenclature

A	Cross-sectional area of cylindrical container, m^2
c_p	Specific heat, J/kg·K
h	Convective heat transfer coefficient, $W/m^2·K$
L	Sand layer thickness, m or mm
M	Weight or sand layer weight, kg
MC	Water content
q	Heat flux, W
T	Temperature or sand layer temperature, K
t	Time, s

Greek symbols

δ	Drying rate, $kg/m^2·s$
λ	Thermal conductivity, W/m·K

Subscripts

0	Hot air
con	Convective
eff	Effective
lat	Latent
s	Sand particle
sen	Sensible
w	Water

consumption of drying field accounts for 10%–25% of total industrial energy consumption [7]. If appropriate drying method and condition are chosen, the drying time and energy consumption can be reduced by 17–33.3%, and the drying efficiency can be increased by 33%–39% [8].

Many experimental studies have been done on convective drying of wet porous materials. For examples, Darıcı and Sen [9] experimentally studied the convective drying characteristics of kiwi fruit and found that the kiwi drying rate was influenced more by the air temperature and relative humidity than by the air velocity. Rabha et al. [10] experimentally investigated the drying characteristics of thin layer ghost chilli pepper in a forced convection tunnel and reported that the drying process included only the falling rate period. Lu et al. [11,12] experimentally investigated the convective drying process of a wet bed packed with quartz particles and reported that the bed drying process included the temperature rise period, constant drying rate period and reduced drying rate period.

Our literature survey suggests that the previous experimental studies on porous media convective drying focused mainly on the moisture content changes but paid inadequate attentions to the temperature variation. Also, their air fluid mostly flowed across the sample surface, causing a non-uniform drying of the sample due to the entrance effect, which was often neglected in the data reduction process. In this research, a specially designed experimental setup is used to investigate the convective air-drying of a wet porous sand layer, it allows the dynamic measurements of both sand layer weight and temperature. Experiments are conducted for different air temperatures, and the temperature and drying curves are presented and discussed.

2. Experimental setup and method

Fig. 1 is a schematic diagram of the experimental apparatus used in this research. Air is driven by an axial fan to flow through a duct which has a cross-sectional area of 240 mm × 240 mm and a height of 800 mm, it is heated by an electric heater, mixed by a baffle, and rectified by a flow straightener to form a parallel flow towards the test section. The upper baffle plate has a circular shape whose diameter is 170 mm while the lower baffle plate has a square shape with a circular hole whose diameter is 120 mm. The flow straightener is a perforated

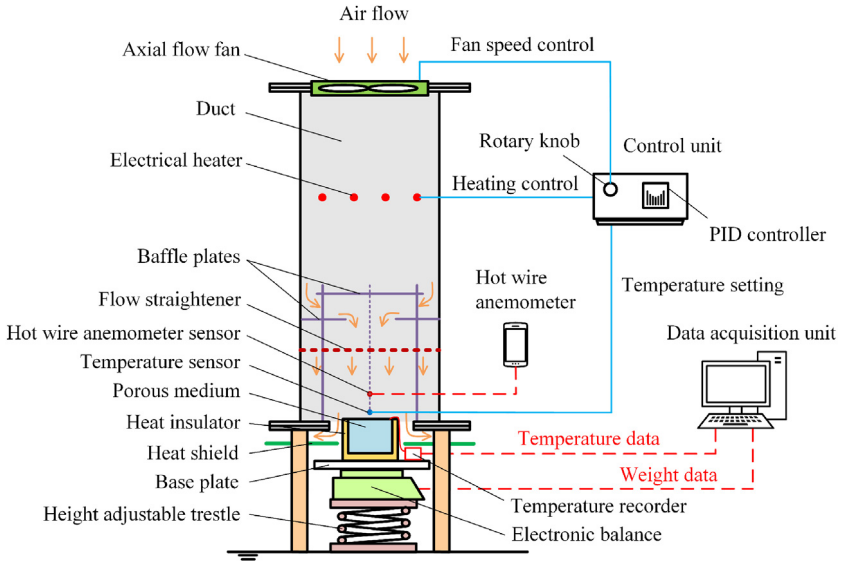

Fig. 1. Schematic diagram of the experimental apparatus.

plate with tremendous small holes. The air velocity is adjusted by a rotary knob and measured by an anemometer (KANOMAX KA23, KANOMAX Inc., Japan, 0–50 m/s measurement range, ±0.1 m/s & ±0.5 °C accuracy), with the air temperature being controlled by a PID controller and measured by a thermistor (Pt100, ±0.1 °C accuracy), whose output is directly imported into the PID controller to realize the air temperature control. The air fluid across the straightener proceeds towards the test section and exits through an annular vent at the duct bottom.

Fig. 2 shows the test section, which includes a cylindrical container (Polystyrene, Ø90×18 mm) containing multiple built-in thermocouples, a wet sand layer made of silica sand (0.19–0.38 mm particle size) and distilled water, as well as some insulators on its outside surface. The thermocouples (T type, 0.1 mm diameter, ±0.1 °C accuracy) are embedded at the positions as indicated in Fig. 2, two of them (TC 1, 2) locate at the axis of the cylinder at the positions of the sand layer surface and bottom while the other two (TC 3, 4) locate at the same vertical positions but 20 mm away from the axis. The container containing the wet sand layer, along with the built-in thermocouples and a temperature recorder, are all placed on an electronic balance, which is supported by a height-adjustable trestle. By altering the trestle height, the container vertical position can be adjusted. In the experiment, the sand layer temperatures are recorded by the temperature recorder (Jinko JK 808, Jinko Electronic Technology Co. Ltd., China, ±0.2% accuracy) while the container assembly total weight is recorded by the electronic balance (BN-V8-1500+S, Uniweight Precision Co. Ltd., China, 0–1500 g measurement range, ±0.01 g accuracy).

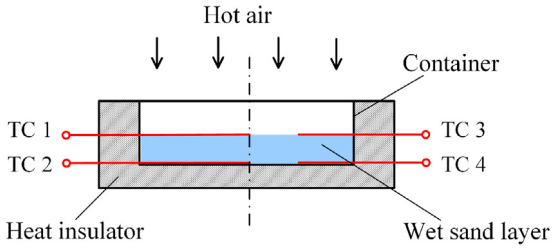

Fig. 2. Test section and thermocouple arrangement.

Experiments are carried out for a 4 mm thick sand layer at atmospheric pressure for three air temperatures of $T_0 = 45$, 60 and 75 °C. The air has a humidity ratio of 0.1 kg/kg, yielding wet bulb temperatures of 22.5, 27.4 and 33.5 °C for $T_0 = 45$, 60 and 75 °C, which can be calculated from the equation given by Min and Tang [13] and Tang

and Min [14]. The air velocity is measured by the anemometer locating 50 mm above the sand layer surface and is maintained at 0.3 m/s throughout the experiment. In each experiment, the weight of the container assembly, which includes the container, the heat insulators attached to the container side and bottom surfaces, the thermocouples glued at the container side wall, as well as the temperature recorder, is first measured and is recorded as M_1. Silica sand is then added to the container until the sand layer reaches a target height, the weight of the container assembly at this time is measured again and is recorded as M_2. After that, distilled water is added to the container using a syringe until the water just submerges the sand layer upper surface to form a fully wet surface, and the weight of the container assembly at this time is measured once again and is recorded as M_3. If the weight of the container assembly during the experiment is expressed as M, the moisture content of the sand layer can be calculated from

$$MC = \frac{M_w}{M_w + M_s} = \frac{M - M_2}{(M - M_2) + (M_2 - M_1)} = \frac{M - M_2}{M - M_1} \tag{1}$$

where M_s and M_w are the weights of silica sand and water, while the initial moisture content can be obtained by replacing M with M_3 in Eq. (1). Also, the drying rate can be computed from

$$\delta = \frac{1}{A}\frac{\Delta M}{\Delta t} = \frac{1}{A}\frac{\Delta M_w}{\Delta t} \tag{2}$$

where A is the cross-sectional area of cylindrical container, Δt is a small time interval, and ΔM and ΔM_w denote the total and water weight decrements corresponding to Δt, they are equal to each other. Each experiment is implemented until the sand layer temperature attains to the hot air temperature and the sand layer temperature and weight become almost unchanged.

3. Results and discussion

Fig. 3 illustrates the variations of sand layer temperature with drying time. For each air temperature, the four temperature curves corresponding to the four thermocouples locating at different places as shown by Fig. 2 all overlap, suggesting that little temperature distribution exists in the sand layer. The sand layer temperature initially increases rapidly, then more gently, which lasts for a relatively long period of time, and eventually increases rapidly again until it reaches a temperature very close to the hot air temperature, it then gradually approaches and finally attains to the hot air temperature. Although the sand layer is completely covered by water at the beginning of the experiment, there is no period at which the sand layer temperature remains constant at the air wet-bulb

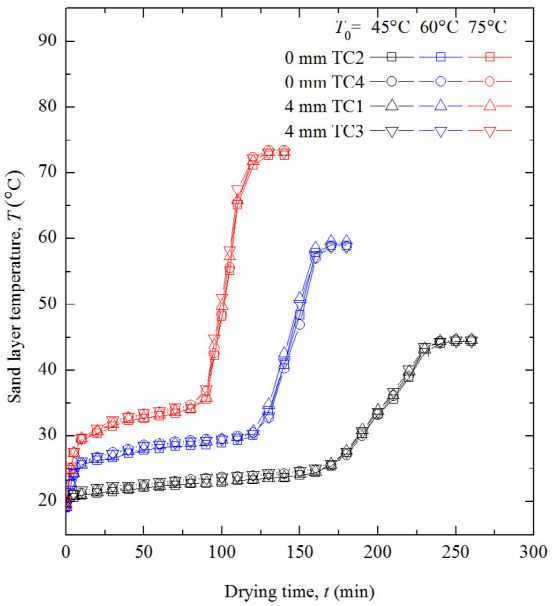

Fig. 3. Variation of sand layer temperature with drying time.

temperature, which was often reported by the other researchers. The reason may be that free water might exist on their sample surfaces for a longer period of time in their experiments. The sand layer temperature continuously increases throughout the drying process in our experiments, implying that the convective heat from the hot air can never be balanced by the latent heat of water evaporation occurring at the sand layer upper surface, there is always some surplus convective heat that is used to increase the sensible heat of the sand layer.

Fig. 4 depicts the variations of sand layer moisture content and drying rate with drying time. For each air temperature, the sand layer moisture content continues to decrease with time, with a higher air temperature giving a shorter drying time. When the air temperature is increased from 45 °C to 75 °C, the drying time decreases from about 250 min to 130 min. Whereas the sand layer drying rate initially increases, then maintains almost constant for a relatively long period of time, and eventually turns to decrease until it attains to zero. So, the drying process contains three stages including the increasing, constant, and decreasing rate stages, which are roughly correspond to the three temperature rise stages as observed in Fig. 3. At the early drying stage, the drying rate increases because the sand layer temperature increases, which acts to increase the saturation specific humidity at the sand layer upper surface, causing a larger mass transfer driving potential between the sand layer upper surface and hot air. At the intermediate drying stage, the sand layer temperature increases while the sand layer upper surface wittedness decreases, the former works to increase the drying rate whereas the latter acts to reduce the drying rate, leading to a nearly constant drying rate. At the late drying stage, the sand layer upper surface becomes fully dry and the evaporation front immerges in the land layer, the resulting dry region appearing in the sand layer upper part acts to increase the moisture transfer resistance, causing a reduced drying rate. Fig. 4b also indicates that a higher air temperature yields a larger drying rate and consequently a shorter drying time.

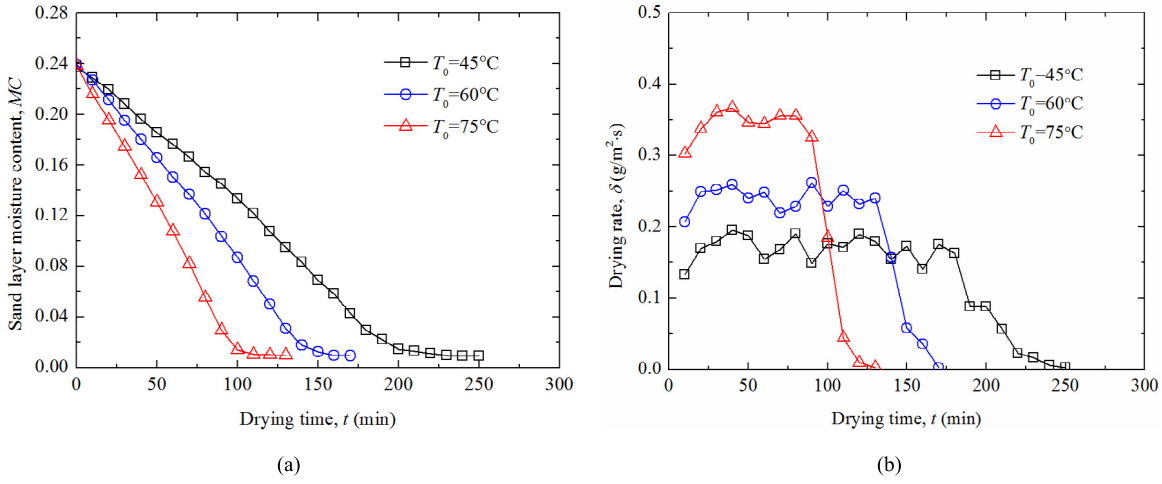

Fig. 4. Variations of sand layer (a) moisture content and (b) drying rate with drying time.

As stated above, little temperature distribution exists in the sand layer, the lumped parameter method can therefore be employed to analyze the sand layer heat transfer. The convective heat from the hot air should be equal to the sum of the latent heat for the water evaporation and the sensible heat for the sand layer temperature rise, i.e.

$$q_{con} = q_{lat} + q_{sen} \tag{3}$$

$$q_{con} = h\,(T_0 - T) \tag{4}$$

$$q_{lat} = \frac{1}{A} h_{vap} \frac{\Delta M_w}{\Delta t} \tag{5}$$

$$q_{sen} = \frac{1}{A}\left(c_{p,s} M_s + c_{p,w} M_w\right) \frac{\Delta T}{\Delta t} \tag{6}$$

where h is the convective heat transfer coefficient, T is the sand layer temperature, $c_{p,s}$ is the specific heat of silica sand, which has a value of 0.837 kJ/kg, M_s is the weight of silica sand, and M_w is the weight of water. Since the water weight decreasing rate ($\Delta M_w/\Delta t$) is available from Fig. 4b, the latent heat (q_{lat}) can be calculated from Eq.

(5); Further, since the water weight (M_w) and sand layer temperature increasing rate ($\Delta T/\Delta t$) are available from Figs. 4a and 3, the sensible heat (q_{sen}) can be computed from Eq. (6). When the latent and sensible heats are known, the convective heat (q_{con}), which is the sum of the latent and sensible heats, can be obtained from Eq. (3). Fig. 5a illustrates the evolutions of the abovementioned various heats. The latent heat shows a variation similar to that of the drying rate as shown in Fig. 4b, they both are proportional to the water weight decreasing rate ($\Delta M_w/\Delta t$), as seen in Eqs. (5) and (2). The sensible heat is much smaller than the latent heat, it gives relatively large values at the initial and final drying stages, which correspond to the sand layer temperature rapid increase stages as indicated in Fig. 3. As a result, the convective heat is nearly equal to the latent heat over most of the drying process. Based on the convective heat and sand layer temperature shown in Figs. 4a and 3, the convective heat transfer coefficient can be calculated from Eq. (4), with the obtained result being presented in Fig. 5b, which shows that the convective heat transfer coefficient is roughly at a level of 20 W/m^2 K except in the period in which the drying is nearly finished.

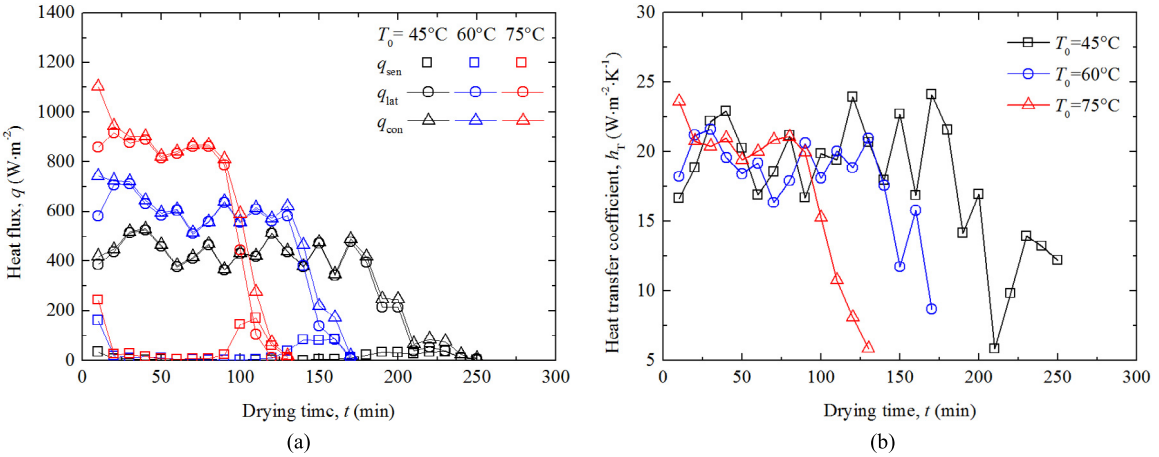

Fig. 5. (a) Various heats; (b) Convective heat transfer coefficient.

The Biot number is usually used to judge if the lumped parameter method can be adopted to analyze the combined convective and conductive heat transfer. In this research, the heat transfer Biot number can be calculated using Eq. (7), in which h_{sen} is the equivalent convective heat transfer coefficient corresponding to the sensible heat, defined by Eq. (8), and L and λ_{eff} are the thickness and effective thermal conductivity of the sand layer. By using Eq. (15) in [5] and taking the sand particle thermal conductivity as 1.3 W/m K, the sand layer effective thermal conductivity can be calculated to be 0.91 W/m K for the case that the pores in the sand layer are full of water, which is close to the situation at the beginning of the drying, and 0.37 W/m K for the case that the pores are full of gas, which is close to the situation at the end of the drying. Fig. 6 depicts the variations of the equivalent heat transfer coefficient, which has a small value of about 0.3 W/m^2 K at the intermediate drying stage, which corresponds to the slow temperature rise stage, and a large value of about 7 W/m^2 K at the final drying stage, which corresponds to the second temperature rapid rise stage. So, the Biot number can be estimated to be $0.3 \times 0.004/[(0.91 + 0.37)/2] = 0.0019$ for the intermediate drying stage, and $7 \times 0.004/0.37 = 0.0757$ for the final drying stage. Since $Bi < 0.01$ is usually thought to be a criterion for use of the lumped parameter method, the method may not apply to the final drying stage, during which the thermocouples locating at different places did give notably different temperatures as observed in Fig. 3.

$$Bi = h_{sen}L/\lambda_{eff} \tag{7}$$

$$h_{sen} = q_{sen}/(T_0 - T) \tag{8}$$

4. Conclusions

- The sand layer temperature continuously increases throughout the drying process, which can be divided into three stages, i.e. the initial rapid, intermediate slow, and final rapid increase stages, there is no stage at which the sand layer temperature remains constant at the air wet-bulb temperature.

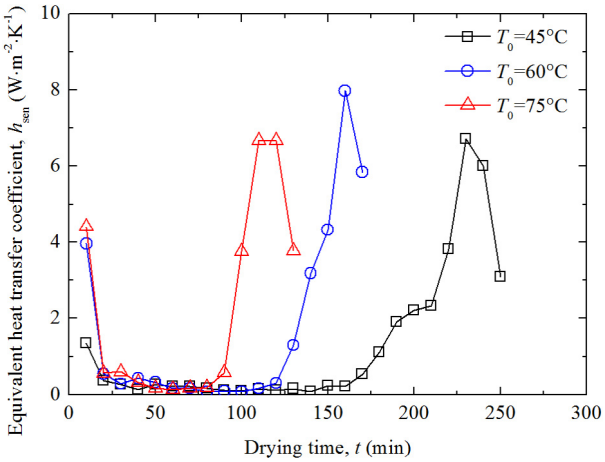

Fig. 6. Equivalent convective heat transfer coefficient corresponding to the sensible heat.

- The sand layer drying process can be divided into three stages according to the sand layer drying rate variation, they are the increasing, constant, and decreasing rate stages, which roughly correspond to the three temperature rise stages.
- The lumped parameter method is adopted to analyze the sand layer heat transfer, and the results support that the convective heat from the hot air is used mainly for the water evaporation, with comparable convective heat transfer coefficients for different air temperatures.
- The heat transfer Biot number is estimated by introducing an equivalent heat transfer coefficient corresponding to the sensible heat, and the results suggest that the Biot number is very small at the intermediate drying stage, which corresponds to the slow temperature rise stage, but it becomes quite large at the final drying stage, which corresponds to the second temperature rapid rise stage. So, the lumped parameter method applies better to the intermediate drying stage than to the final drying stage.

Acknowledgment

This study is funded by National Natural Science Foundation of China through Grant No. 51376103.

References

[1] Bear Jacob. Dynamics of fluids in porous media. New York: Elsevier; 1972.
[2] Pourrahmani Hossein, Moghimi Mahdi, Siavashi Majid. Thermal management in PEMFCs: The respective effects of porous media in the gas flow channel. Int J Hydrogen Energy 2019;44:3121–37.
[3] Khan Furqan Ahmad, Straatman Anthony Gerald. A conjugate fluid-porous approach to convective heat and mass transfer with application to produce drying. J Food Eng 2016;179:55–67.
[4] Tang Yicun, Min Jingchun, Wu Xiaomin. Selection of convective moisture transfer driving potential and its impacts upon porous plate air-drying characteristics. Int J Heat Mass Transfer 2018;116:371–6.
[5] Tang Yicun, Min Jingchun. Water film coverage model and its application to the convective air-drying simulation of a wet porous medium. Int J Heat Mass Transfer 2019;131:999–1008.
[6] Castro AM, Mayorga FL, Moreno EY. Mathematical modelling of convective drying of fruits: A review. J Food Eng 2018;223:152–67.
[7] Mujumdar Arun S. Handbook of industrial drying. Boca Raton: CRC Press; 2006.
[8] Zhang Min, Chen Huizhi, Mujumdar Arun S, Zhong Qifeng, Sun Jincai. Recent developments in high-quality drying with energy-saving characteristic for fresh foods. Drying Technol 2015;33:1590–600.
[9] Darıcı Selçuk, Sen Soner, Experimental investigation of convective drying kinetics of kiwi under different conditions. Heat Mass Transf 2015;51(8):1167–76.
[10] Rabha DK, Muthukumar P, Somayaji C. Experimental investigation of thin layer drying kinetics of ghost chilli pepper (Capsicum Chinense Jacq.) dried in a forced convection solar tunnel dryer. Renew Energy 2017;105:583–9.
[11] Lu Tao, Jiang Peixue, Shen Shenqiang. Numerical and experimental investigation of convective drying in unsaturated porous media with bound water. Heat Mass Transf 2005;41(12):1103–11.
[12] Lu Tao, Shen Shengqiang, Liu Xiaohua. Numerical and experimental investigation of heat and mass transfer in unsaturated porous media with low convective drying intensity. Heat Transfer-Asian Res 2008;37(5):290–312.

[13] Min Jingchun, Tang Yicun. Theoretical analysis of water film evaporation characteristics on an adiabatic solid wall. Int J Refrig 2015;53:55–61.
[14] Tang Yicun, Min Jingchun. Evaporation characteristics analysis of water film on a spherical solid particle. Appl Therm Eng 2016;102:539–47.